Development of Advanced Tritium Breeders and Neutron Multipliers for DEMO Solid Breeder Blankets

K. Tsuchiya 1), T. Hoshino 1), H. Kawamura 1), Y. Mishima 2), N. Yoshida 3), T. Terai 4), S. Tanaka 4), K. Munakata 3), S. Kato 5), M. Uchida 6), M. Nakamichi 1), H. Yamada 1), D. Yamaki 1), K. Hayashi 1)
1) Japan Atomic Energy Agency (JAEA), Ibaraki-ken, Japan.
2) Tokyo Institute of Technology, Kanagawa-ken, Japan
3) Kyushu University, Fukuoka-ken, Japan
4) The University of Tokyo, Tokyo, Japan
5) Nuclear Fuel Industries, Ltd., Ibaraki-ken, Japan
6) NGK INSULATORS, LTD., Aichi-ken, Japan
E-mail: tsuchiya.kunihiko@jaea.go.jp

In efforts to develop advanced tritium breeders, effects of additives to lithium titanate (Li_2TiO_3) have been investigated, and a good prospect has been obtained by using oxide additives such as TiO_2, CaO and Li_2O. As for neutron multiplier, development of a real-size electrode fabrication technique and the characterization of beryllium-based intermetallic compounds such as Be-Ti have been performed. The properties of Be-Ti alloys are better than those of beryllium metal. Especially, steam interaction of a Be-Ti alloy was about 1/1000 as small as those of beryllium metal. These activities have given bright prospects to realize the water-cooled DEMO breeder blanket by application of these advanced materials.

1. Introduction

The design of advanced fusion blanket with ferrite steels (F82H) as the structural material has been studied to realize DEMO reactors in Japan [1]. In the design under development, the coolant temperature is above 500˚C, and it is required for the tritium breeder and neutron multiplier in the blanket to accommodate the high temperature and high neutron fluence.

For the tritium breeder, lithium titanate (Li_2TiO_3) pebbles with a diameter were chosen as a tentative reference material from viewpoints of good tritium recovery at low temperature, low tritium inventory and chemical stability [2-3]. Concerning a pebble fabrication method, it has been clarified that the specification target (density: 80-85%T.D., grain size: <5μm) of tritium breeder was reached by a wet process [4]. In order to study the tritium release behavior, in-situ tritium recovery experiments with Li_2TiO_3 pebbles were carried out at the Japan Materials Testing Reactor (JMTR) [5]. Although Li_2TiO_3 showed favorable results at low irradiation temperatures, it also became clear that its stability at high temperatures is not satisfactory. Therefore, Li_2TiO_3 added with oxide has been developed as advanced tritium breeders and the characteristics of this material were evaluated.

For the neutron multiplier, beryllium (Be) metal is a reference material in the blanket design [6]. However, it may not be applicable to the DEMO blanket that requires high temperature (~900˚C) and high neutron dose (~20,000appmHe, ~50dpa). Therefore, it is necessary to develop an advanced material that has high temperature resistance and high radiation resistance. Beryllides such as $Be_{12}Ti$ and $Be_{12}V$ have been proposed as promising candidates for advanced neutron multipliers from the viewpoints of high melting point, high beryllium content, fast decay of gamma dose rate and good chemical stability [7]. In this paper, several properties studied on Be-Ti alloy with $Be_{12}Ti$ and αBe have been summarized to confirm the advantage.

2. Advanced Ceramic Tritium Breeder

2.1 Effect of oxide in Li_2TiO_3

Lithium titanate (Li_2TiO_3) added with TiO_2 (designated Ti-Li_2TiO_3) was first examined, and characterization of this sample showed that hydrogen reduction ($Ti^{4+} \rightarrow Ti^{3+}$) of a part of titanium in Ti-Li_2TiO_3 was induced easily at temperatures above 800˚C. Therefore, in attempts find better additives, Li_2TiO_3 powder was mixed with a small amount of other oxide additives (CaO, ZrO_2 and Sc_2O_3) [8]. The samples were prepared as Ca-Li_2TiO_3 (CaO/Li_2TiO_3=0.20mol%), Zr-Li_2TiO_3 (ZrO_2/Li_2TiO_3=0.44mol%) and Sc-Li_2TiO_3 (Sc_2O_3/Li_2TiO_3= 0.40mol%), respectively.

In the thermogravimetry of each sample in the temperature range from 200 to 1000˚C (see Fig.1), the weight of sample slightly decreased, generating O-vacancy by reduction at temperature above about 300˚C, and the weight decreased quickly with an enhanced reduction above about 800˚C. Further, Ca-Li_2TiO_3 has fewer oxygen defects than the other kinds of additive-Li_2TiO_3. Ca-Li_2TiO_3 has the smallest mass of TiO_2 in Li_2TiO_3, so that the order of oxygen defects was Ca-Li_2TiO_3 < Li_2TiO_3 ≒ Zr-Li_2TiO_3 < Sc-Li_2TiO_3.

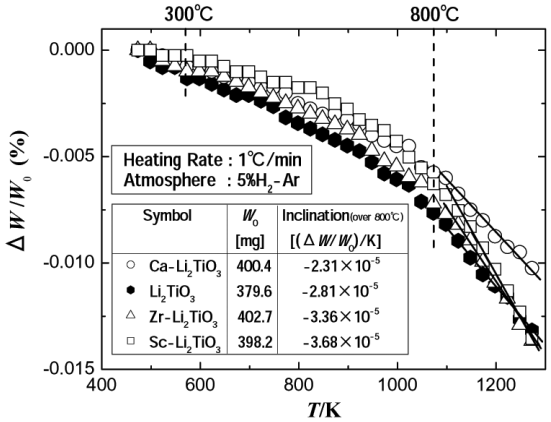

FIG.1 Temperature dependence of the weight change of Li_2TiO_3 with oxide additives in reduction atmosphere.

The vaporization characteristics of non-stoichiometry of Li_2TiO_3 (Li_2O/TiO_2=1.00), Ca-Li_2TiO_3 (CaO/Li_2TiO_3=0.20mol%) and Li-Li_2TiO_3 (Li_2O/TiO_2=1.05) have been extensively investigated by means of atmosphere-controlled high-temperature mass spectrometry [9].

An atmosphere-controlled high-temperature mass spectrometer has provided the vapor pressure data for Li_2TiO_3, Ca-Li_2TiO_3 and Li-Li_2TiO_3, under conditions of D_2 atmospheres. The pressure of Li-containing species (P_{Li}^{total}) over Li_2TiO_3 with oxide additives under the conditions of D_2 atmospheres is shown in Fig.2. The pressure of Li-containing species decreased in the following order;

Ca- Li_2TiO_3 > Li-Li_2TiO_3 > Li_2TiO_3 (1093~1473K)

Li-Li_2TiO_3 ≒ Li_2TiO_3 (<1093K).

This result shows that the Li_2O additives are able to control not only the amount of oxygen defects but also the amount of Li loss, because of Li-Li_2TiO_3 contained more lithium than Li_2TiO_3. It is concluded that the CaO and Li_2O additives are able to control not only the growth of the grain size but also the amount of lithium defects.

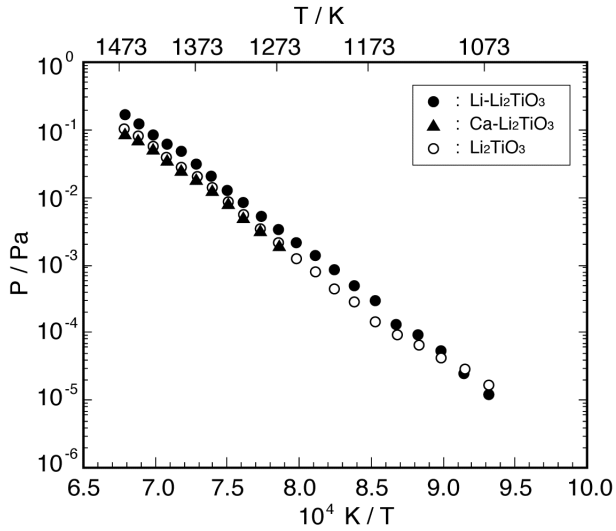

FIG.2. Vapor pressures of Li-containing species (P_{Li}^{total}) over Li_2TiO_3 with oxide additives under the conditions of D_2 atmospheres.

2.2 Irradiation Effects of tritium breeder

Simulation of the fusion reactor environment and the study of the effect of atomic displacement damage in Li_2TiO_3 are presumed to be approached by a simultaneous irradiation of triple ion beams which consist of O^{2+}, He^{+} and H^{+} ion beams [10]. In comparison with the Raman spectra of irradiated Li_2TiO_3 samples for each single ion beam and the reference spectra of Li_2TiO_3 and TiO_2, it has been clarified that the Raman spectra of Li_2TiO_3 samples irradiated with the single H^{+} ion beam or the single He^{+} ion beam are quite similar to the spectrum of un-irradiated Li_2TiO_3, while the spectrum of the sample irradiated with the single O^{2+} ion beam seems to be a superposition of the spectra of Li_2TiO_3 and TiO_2. It is suggested that the formation of TiO_2 on the surface of Li_2TiO_3 observed in the sample irradiated with triple ion beams is mainly caused by the O^{2+} ion beam irradiation.

Using the FT-IR photoacoustic spectroscopy (PAS) technique, un-irradiated samples, the samples irradiated with the triple ion beam and the samples irradiated by the single ion beams were examined in order to obtain information near the end of the ion range. Figure 3 shows the relation between dpa and the 780 cm^{-1} peak area attributable to the Ti-O bond for each irradiation. To simulate the formation of TiO_2 in Li_2TiO_3, samples of Li_2TiO_3 doped with 1-10% TiO_2 were prepared. Comparison of the results from the irradiated and the doped samples suggested that TiO_2 observed by Raman spectroscopy in the sample irradiated with the triple ion beams is formed by atomic displacements, and that the amount of TiO_2 is proportional to the dpa in the sample.

On the other hand, surface analysis of Li_2TiO_3 subjected to Ar^{+} sputtering, heating or water vapor exposure was performed by X-ray/ultraviolet photoelectron spectroscopy (XPS/UPS) [11]. Results of the surface analysis suggested that no absorption of hydroxyl group (-OH) occurred by 5×10^{-13} Pa H_2O exposure of a Li_2TiO_3 specimen subjected to Ar^{+} sputtering with subsequent annealing at 400˚C. However, dissociative (-OH) adsorption was observed for reduced surface created by Ar^{+} sputtering via selective sputtering of Li and O.

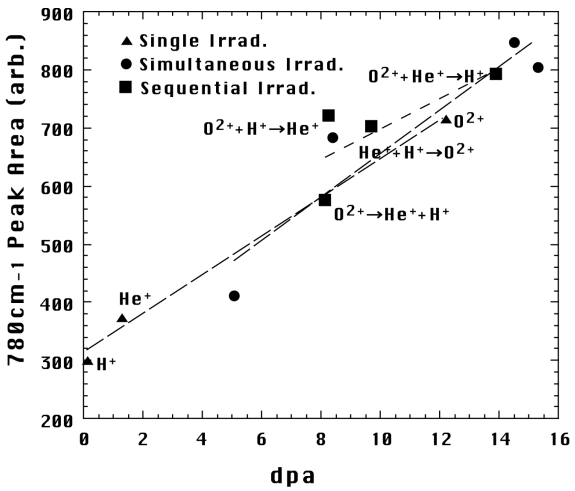

FIG.3 Dependence of the 780cm^{-1} peak area on dpa. Notation for the sequential irradiation as "A→B" means that irradiation of beam B was performed after irradiation of beam A.

3. Advanced Neutron Multiplier

3.1 Fabrication technology development

As the first step, pebbles consisting of Be-Ti alloys were obtained by a small-scale rotating electrode method (REM) [7]. As the next step, fabrication tests of ingot by induction melting and vacuum casting have been carried out to fabricate a real-size electrode. By the previous examinations, information on the conditions causing solidification defects of shrinkage and cracks as well as contamination from the mold has been obtained, which are important to enable economical production of the electrode by induction melting and vacuum casting [12].

Based on the results, further demonstration to fabricate the electrode was carried out. As screening test, four kinds of small ingots ($\phi 70 \times^{h} 150$mm) with Be-7at%Ti, Be-7.7at%Ti, Be-9at%Ti and Be-10.5at%Ti were melt and cast. And Be-7.7at%Ti and Be-10.5at%Ti showed better results.

On the other hand, two kinds of large ingots (dimension: $\phi 200 \times^{h} 400$mm, chemical compositions: Be-7.7at%Ti and Be-10.5at%Ti) were fabricated and characterized. Actual chemical compositions of each ingot were Be-8.1at%Ti and Be-11.3at%Ti, respectively. Casting mold had an iron chill on the bottom to improve shrinkage crack. Large shrinkage exists on the top of ingot, but some good portion was obtained near the bottom.

3.2 Mechanical property of Be-Ti alloys

Temperature dependence of compressive 0.2% flow stress, as expressed by specific strength, of Be-7.7at%Ti and Be-9.0at%Ti fabricated by arc melting is shown in Fig.4. The specific strength at 927˚C of Be-8.1at% Ti alloy (K077) fabricated by the casting method in the present work is also shown in the figure. This figure clearly shows that the alloy exhibits the highest strength at the temperature as compared to other Be-Ti alloys and IN738LC. It is noted that the strength of the Be-Ti alloys at room temperature are the fracture stress, which means that the alloys is brittle exhibiting zero plastic strain at lower temperature. A creep test was also carried out for Be-8.1at%Ti ingot.

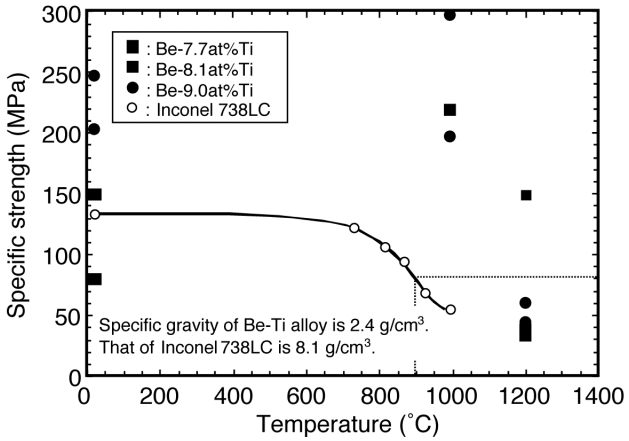

FIG.4 Relationship between temperature and specific strength of Be-Ti alloys.

3.3 Chemical properties of Be-Ti alloys

3.3.1 Compatibility

The compatibility test of Be-Ti alloys (Ti content : 3, 5 and 7at%) was carried out with F82H at 600, 700 and 800˚C up to 1000h. Observation of the reaction and diffusion layers were performed on the F82H side after compatibility tests of Be-Ti alloys and F82H. The thickness of the reaction layer was smaller than that between Be and F82H after annealing. Deficiency of Be was observed on the Be-Ti alloy side, but no reaction layers was observed.

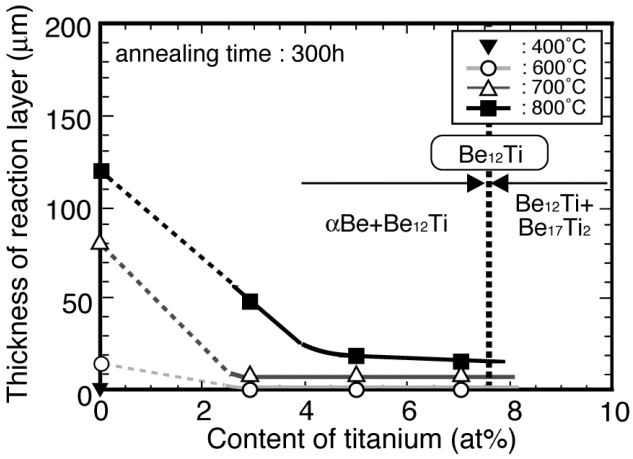

FIG. 5 Relationship between content of titanium in Be-Ti alloys and thickness of reaction layer.

Figure 5 shows the relationship between the content of titanium and the thickness of the reaction layer. The thickness decreases with increasing the content of Ti in Be-Ti alloys. It is considered that $Be_{12}Ti$ is hardly chemically reactive with F82H and that the content of $Be_{12}Ti$ in Be-Ti alloys increases with increasing the Ti content up to a Ti content of 7at%. It is obvious that the compatibility between Be-Ti alloys and F82H is much better than that between Be and F82H [13].

3.3.2 Oxidation resistance

Oxidation property of Ti-beryllides was very good at 800˚C under an atmosphere of dry air [14]. The basic oxidation behavior of Be, Ti and Be-Ti at 1000˚C would be almost the same

as that at 800˚C, because the tendency of the mass gain curves of Be and Ti is the same as that at 800˚C. The mass gain curves of Be-7.7at%Ti, Be-9.0at%Ti and Be-10.5at%Ti alloy were almost flat, and all the mass gains were within 20 gm^{-2} at 24h. Surface appearance of the oxidized samples showed that there was thin, dark gray film on all of the samples. The film is thought to be oxides of Be and/or Ti, and the thickness of them would be about 100 nm, concerning of the very small mass gains and the nominal densities of BeO and TiO_2. This observation suggests that the oxide film formed on the Ti-beryllides has a protective nature, which supports the high oxidation resistance at high temperature.

3.3.3 Steam interaction

Chemical stability of $Be_{12}Ti$ was investigated under the stream of argon gas containing water vapor of 1% [15]. Figure 6 shows changes in the concentration of H_2 in outlet stream of the reactor when the argon gas containing 1% of H_2O was introduced. The generation of H_2 started at a temperature close to 600˚C. The concentration of H_2 in the outlet stream of the reactor reached a peak at 1000˚C and then began to decrease. The generation of H_2 terminated at 10 h and the generation rate was $6.7x10^{-4}$ $l/m^3/s$. The results shows that the steam reaction rate of $Be_{12}Ti$ was about 1/1000 smaller than that of Be.

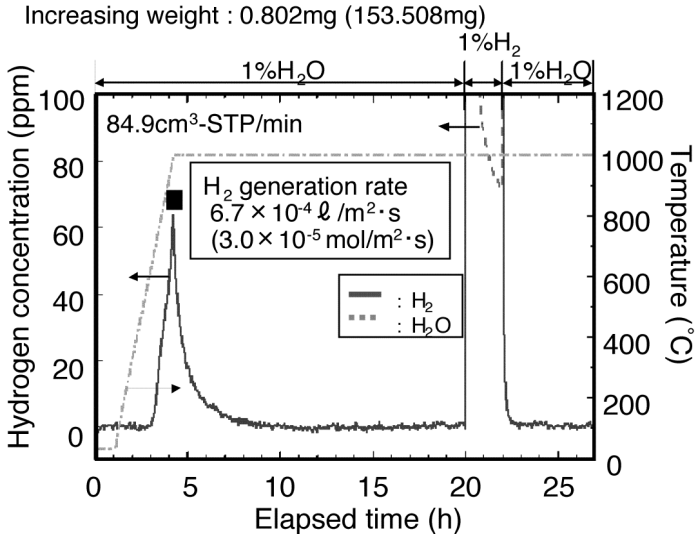

FIG. 6 Change in the concentration of H_2 in the outlet stream of reactor with a $Be_{12}Ti$ disk exposed to 1%H_2O/Ar gas.

The kinetics of oxidation on the surface of $Be_{12}Ti$ by water vapor was examined using a model. The values of activation energy of the oxidation reaction and the amount of the final amount of BeO on the unit surface area were 240 kJ/mol and 0.133 mol/m^2, respectively. To clarify the mechanism of the high tolerance of $Be_{12}Ti$ to water vapor, surface observation of the sample was performed by means of digital microscope, SEM, XRD and ESCA. The results suggest that some oxidized layer is present on the surface of the sample. In particular, observation by ESCA gave some clues to understand the higher tolerance of $Be_{12}Ti$ to water vapor at high temperatures.

3.4 Tritium inventory

Thermal desorption of deuterium from $Be_{12}Ti$ irradiated by D_2^+ ions and microstructural change during irradiation were examined to understand deuterium retention and desorption properties [16].

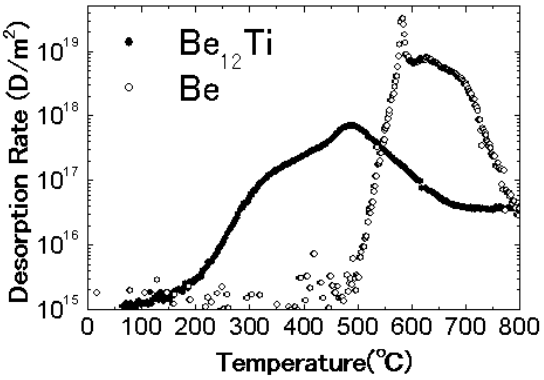

FIG. 7 Thermal desorption of deuterium gas from Be and $Be_{12}Ti$ irradiated with deuterium ions. (Temperature ramping rate: 1 K/sec)

Figure 7 shows thermal desorption spectra of deuterium from $Be_{12}Ti$ and beryllium with 8 keV-D_2^+ to dose of $2x10^{21}$ D^+/m^2 at 400˚C. In the case of beryllium, deuterium retention is much larger than that of $Be_{12}Ti$; 66% of implanted deuterium is retained and most of this is desorbed between 550 and 750˚C. A large number of long peculiar defects suitable for uniaxial direction were observed in beryllium by transmission electron microscopy, and these defects were three-dimensional cavities. In the $Be_{12}Ti$, no defect was observed in this irradiation condition. This fact indicates that nucleation of cavities is not easy in this irradiation condition. Deuterium trapping sites are supposed to very small vacancy clusters (<2nm) and impurities. It seems reasonable to suppose from the results that low swelling and low hydrogen isotope retention under neutron irradiation can be expected at elevated temperatures above 327˚C.

3.5 Irradiation effects of neutron multiplier

The synergistic effects of helium transmutation and irradiation damage on microstructure evolution in pure Be and $Be_{12}Ti$ have been studied by in-situ observation under fusion equivalent environments using Multi Beam High Voltage Electron Microscope (MB-HVEM). After electron-He ion dual beam irradiation to $2.15x10^{22}$ e/cm^2 with $1.40x10^{15}$ He ions/cm^2 at R.T., many bubbles were observed in pure Be. However, less bubble formation was observed in $Be_{12}Ti$. As increasing the irradiation temperature to 500˚C at the same irradiation dose, still less bubble formation was observed in $Be_{12}Ti$. But, some tiny bubbles were observed along the-sub grain boundary in $Be_{12}Ti$. However, it was hard to observe black dots or dislocation loops associated with radiation induced interstitials in $Be_{12}Ti$ under other diffraction conditions. This result suggested that interstitial would be immobile due to the complex crystallographic structure of $Be_{12}Ti$ in this experimental condition.

4. Conclusions

The advanced materials of tritium breeder and neutron multiplier with high temperature

resistance have been developed, and good prospect to realize the DEMO breeding-blanket has been obtained by the application of Li_2TiO_3 added with oxide such as TiO_2, CaO and Li_2O, and by adopting Be alloys containing beryllium intermetallic compounds.

Ackowledgement

A part of the present work (part of Section 3.1, 3.2 and 3.3.2) is being supported by a grant-in-aid for International Collaborative Environmental Project from New Energy and Industrial Technology Development Organization (NEDO) of Japan.

References

[1] ENOEDA, M., et al., "Development of solid breeder blanket at JAERI", *Fusion Science and Technology*, **47** (2005) 1060.
[2] GIERSZEWSKI, P., "Review of properties of lithium metatitanate", *Fusion Eng. Des.*, **39-40** (1998) 739.
[3] KAWAGOE, T. et al., "Surface inventory of tritium on Li_2TiO_3", *J. Nucl. Mater.*, **297** (2001) 27.
[4] TSUCHIYA, K., et al., "Control of particle size and density of Li_2TiO_3 pebbles fabricated by indirect wet process", *J. Nucl. Mater.*, **345** (2005) 239.
[5] TSUCHIYA, K., et al., "In-situ tritium recovery experiments of blanket in-pile mockup with Li_2TiO_3 pebble bed in Japan", *J. Nucl. Sci. Technol.*, **38** (2001) 996.
[6] KAWAMURA, H. and OKAMOTO, M. (Eds.), "Proc. 3rd IEA International Workshop on Beryllium Technology for Fusion, October 22-24, 1997, Mito, Japan", JAERI-Conf 98-001.
[7] KAWAMURA, H., et al., "Present status of beryllide R&D as neutron multiplier", *J. Nucl. Mater.*, **329-333** (2004) 112.
[8] HOSHINO, T., et al., "Non-stoichiometory of Li_2TiO_3 under hydrogen atmosphere condition", *Fus. Eng. Des.*, **75-79** (2005) 939.
[9] HOSHINO, T., et al., "Vapor species evolved from Li_2TiO_3 heated at high temperature under various conditions", *Fus. Eng. Des.*, **81** (2006) 555.
[10] YAMAKI, D., et al., "Observation of the microstructural changes in lithium titanate by multi-ion irradiation", *J. Nucl. Mater.*, 329-333 (2004)1279.
[11] OLIVARES, R. U., et al., "Behavior of Li_2TiO_3 under varied surface condition", *Fus. Eng. Des.*, **75-79** (2005) 765.
[12] MISHIMA, Y., et al., "Recent results on Beryllium and Beryllides in Japan", 12th International Conference on Fusion reactor Materials, Santa Barbara, CA, USA, Dec. 4-9 (2005), to be published in *J. Nucl. Mater.*
[13] TSUCHIYA, K., et al., "Compatibility between Be-Ti alloys and F82H steel", 12th International Conference on Fusion reactor Materials, Santa Barbara, CA, USA, Dec. 4-9 (2005), to be published in *J. Nucl. Mater.*
[14] SATO, Y., et al., "High temperature oxidation behavior of titanium beryllide in air", Proc. of the 6th IEA International Workshop on Beryllium Technology for Fusion Miyazaki, Japan, Dec. 2-5 (2003), JAERI-Conf 2004-006, p.203.
[15] MUNAKATA, K., et al., "Surface reaction of titanium beryllide with water vapor", Fus. Eng. Des., 81 (2006) 993.
[16] IWAKIRI, H., et al., "Deuterium retention properties of $Be_{12}Ti$", Proc. of the 6th IEA International Workshop on Beryllium Technology for Fusion Miyazaki, Japan, Dec. 2-5 (2003), JAERI-Conf 2004-006, p.220.